



HAL
open science

On the Control of a One Degree-of-Freedom Juggling Robot

Bernard Brogliato, Arturo Zavala-Río

► **To cite this version:**

Bernard Brogliato, Arturo Zavala-Río. On the Control of a One Degree-of-Freedom Juggling Robot. Dynamics and Control, 1999, 9 (1), pp.67-91. 10.1023/A:1008346825330 . hal-02303974

HAL Id: hal-02303974

<https://hal.science/hal-02303974>

Submitted on 2 Oct 2019

HAL is a multi-disciplinary open access archive for the deposit and dissemination of scientific research documents, whether they are published or not. The documents may come from teaching and research institutions in France or abroad, or from public or private research centers.

L'archive ouverte pluridisciplinaire **HAL**, est destinée au dépôt et à la diffusion de documents scientifiques de niveau recherche, publiés ou non, émanant des établissements d'enseignement et de recherche français ou étrangers, des laboratoires publics ou privés.

On the Control of a One Degree-of-Freedom Juggling Robot

A. ZAVALA-RÍO

zavala@lag.ensieg.inpg.fr

Laboratoire d'Automatique de Grenoble (UMR 5528 CNRS-INPG), ENSIEG, BP 46, 38402 St. Martin d'Hères, France

B. BROGLIATO

brogli@lag.ensieg.inpg.fr

Laboratoire d'Automatique de Grenoble (UMR 5528 CNRS-INPG), ENSIEG, BP 46, 38402 St. Martin d'Hères, France

Abstract. This paper is devoted to the feedback control of a one degree-of-freedom (dof) juggling robot, considered as a subclass of mechanical systems subject to a unilateral constraint. The proposed approach takes into account the whole dynamics of the system, and focuses on the design of a force input. It consists of a family of hybrid feedback control laws, that allow to stabilize the object around some desired (periodic or not) trajectory. The closed-loop behavior in presence of various disturbances is studied. Despite good robustness properties, the importance of good knowledge of the system parameters, like the restitution coefficient, is highlighted. Besides its theoretical interest concerning the control of a class of mechanical systems subject to unilateral constraints, this study has potential applications in non-prehensile manipulation, extending pushing robotic tasks to striking-and-pushing tasks.

Keywords: nonsmooth mechanical systems, juggling, hybrid control, robustness, viability, non-prehensile manipulation

1. Introduction

The feedback control of mechanical systems subject to unilateral constraints has received some attention. However, it remains largely unexplored. Recent research concerning analysis and control of such nonsmooth systems has focused on stabilization of manipulators [4], [14], wellposedness and system theoretical issues [33], [34], bipedal locomotion [10], [16], control of juggling and catching robots [1], [5], [6], [7], [22], [23], [24], [25], [26], [27], [28], [29], [35], [36], [37], [38], stabilization of polyhedral objects in some manipulation tasks [43], non-prehensile manipulation [11], [15], [19], [21]. One common feature of these studies is that the open-loop models used are basically rigid body dynamics with a set of unilateral constraints on the generalized position. Such systems may be represented as follows:

$$M(q)\ddot{q} + C(q, \dot{q})\dot{q} + g(q) = Tu + \nabla_q f(q, t)\lambda \quad (1)$$

$$f(q, t) \geq 0 \quad (2)$$

$$\lambda \geq 0 \quad , \quad \lambda^T f(q, t) = 0 \quad (3)$$

where the classical dynamics of Lagrangian systems is in (1), the set of unilateral constraints is in (2) with $f(q, t) \in \mathbb{R}^\ell$, and the so-called complementarity conditions [34] are in (3) where $\lambda \in \mathbb{R}^\ell$ is the Lagrange multiplier vector. We assume frictionless constraints, although this assumption is worthless concerning the one dof juggler (impacts are always central). $q \in \Phi \triangleq \{q \in \mathbb{R}^n : f(q, t) \geq 0\}$, $M(q) \in \mathbb{R}^{n \times n}$, $C(q, \dot{q})\dot{q} \in \mathbb{R}^n$, $g(q) \in \mathbb{R}^n$ and $u \in \mathbb{R}^m$ are the generalized coordinate vector, the inertia matrix, the Coriolis and centrifugal terms, the gravity forces and torques, and the control input respectively, with $T \in \mathbb{R}^{n \times m}$. In order to render the dynamical system complete, one must add to (1)–(3) a so-called restitution law that relates post and preimpact velocities. Such physical rules are necessary to render the domain Φ invariant with respect to the system’s dynamics. The most widely used restitution rule is known as Newton’s conjecture [2]. It is based on the knowledge of restitution coefficients e_i , and is represented in its generalized form as follows:

$$\dot{q}(t_k^+)^T \nabla_q f_i(q(t_k), t_k) = -e_i \dot{q}(t_k^-)^T \nabla_q f_i(q(t_k), t_k) - (1 + e_i) \nabla_t f_i(q(t_k), t_k) \quad (4)$$

where $\nabla_q f_i \in \mathbb{R}^n$, $1 \leq i \leq \ell$, and t_k generically denotes the impact times (the superindices $+$ and $-$ stand respectively for the instants just after and just before the collisions), with $\dot{q}(t_k^-)^T \nabla_q f_i(q(t_k), t_k) < 0$. In case of a codimension 1 constraint ($\ell = 1$), $e \in [0, 1]$ from energetical arguments. The system in (1)–(4) is complete, in the sense that given preimpact velocities $\dot{q}(t_k^-)$, one is able to calculate the postimpact velocities and continue the integration after the collision has occurred. Let us notice that the system in (1)–(4) is a complex hybrid dynamical system [3]. This class of dynamical systems can be divided further into subclasses. In particular the case when the free-motion dynamics are controllable has recently received attention [4], [33]. However this class does not cover some impacting robotic systems like bipedal and juggling robots. Indeed let us write down the dynamical equations of a one dof juggler, i.e., a system composed of an object (a ball) subject to gravity, which rebounds on a controlled mass (a one dof robot) as shown in figure 1:

$$m_1 \ddot{y}_1 = -m_1 g \quad (5)$$

$$m_2 \ddot{y}_2 = -m_2 g + u \quad (6)$$

$$f(y_1, y_2) = y_1 - y_2 \geq 0 \quad (7)$$

$$\dot{y}_1(t_k^+) - \dot{y}_2(t_k^+) = -e [\dot{y}_1(t_k^-) - \dot{y}_2(t_k^-)] \quad (8)$$

The dynamics in (5)–(8) may be seen as a simple convex conical system [32] in the sense that if ϕ_1 and ϕ_2 are continuous-time trajectories of (5)–(8) then $\beta\phi_1 + (1 - \beta)\phi_2$, $\forall \beta \in [0, 1]$, is also a continuous-time trajectory of the system. Most importantly, notice that the ball dynamics in (5) are not controlled since only gravity acts on the ball. Hence, the only way to influence the trajectory (y_1, \dot{y}_1) is through impacts, i.e., at times t_k such that $y_1(t_k) - y_2(t_k) = 0$. This is a strong motivation for considering the feedback control of a one dof juggler as in (5)–(8) since it represents a simplified model of manipulation of objects through “controlled” collisions with a robotic device [43].

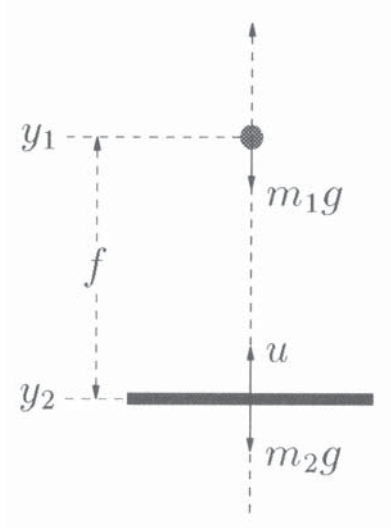


Figure 1. One dof juggler.

Remark 1. More generally, juggling robots may also be considered as a particular case of a class of nonlinear systems:

$$\dot{z}_1 = f_1(z_1, t, \lambda) \quad (9)$$

$$\dot{z}_2 = f_2(z_2, u, \lambda) \quad (10)$$

$$h(q_1, q_2, t) \geq 0, \quad \lambda^T h(q_1, q_2, t) = 0, \quad \lambda \geq 0 \quad (11)$$

where $z_i \triangleq (q_i^T, \dot{q}_i^T)^T \in \mathbb{R}^{2n_i}$, $i = 1, 2$ (n_1 and n_2 may have the same or different values), $u \in \mathbb{R}^m$, $\lambda \in \mathbb{R}^\ell$, and a restitution law must be added to complete the model. Our goal is to stabilize $z_1(t)$ around a desired trajectory. The controllability and stabilizability properties of such systems, which depend on the vector fields in (9), (10) and on h in (11), have not yet been fully understood. However, as we shall see later, some basic properties are quite useful. Among those: *i*) the explicit knowledge of the trajectories of (9) between impacts, *ii*) the controllability of (10), and *iii*) the controllability of (9) through collisions. Property *iii*) will be made clear in remark 5. Interestingly enough, let us note that those assumptions are quite similar to the assumptions made in [17], although the class of nonlinear systems they considered and the control objectives are quite different (they deal with asymptotic stabilization to the origin of a class of smooth cascaded systems modeling nonholonomic mechanisms). The interest for considering systems as in (9)–(11) is that their study finds potential applications in all types of juggling robots, catching tasks, non-prehensile manipulation (pushing-and-striking tasks), and stabilization of manipulators on passive dynamical environments. It is clear that in practice, disturbances and parameter uncertainties will be an obstacle to the use of assumption *i*). Hence, robustness studies will be very important for such systems. Finally, it is worth noting the similarities between systems as in (9)–(11) and walking or hopping machines. Indeed in both cases there is a part of the system that is not controllable during flight times (i.e., the center of mass motion for walking robots). We therefore conjecture that the dynamics in (9)–(11) may represent a very large class of systems subject to unilateral constraints. The role of the vector fields f_1 , f_2 and of h in the stabilizability properties of such systems remains however an open

field, as well as that of the restitution rule¹ (recall that a restitution law must be added to complete the model). The study of simple juggling robots is expected to be a nice manner to investigate their basic properties.

2. Review of Previous Work

The structure of mechanical systems as in (5)–(8) naturally leads to the study of their dynamics and the control design at impact times only through their so-called impact Poincaré map P_Σ (the Poincaré section is chosen as $\Sigma = \{(q, \dot{q}, t) \in \Phi \times \mathbb{R}^n \times \mathbb{R}_+ : f(q, t) = 0, \dot{q}^T \nabla_q f(q, t) > 0\}$). One way to obtain the closed-loop impact Poincaré map is to integrate (5) and (6) between impacts to get

$$y_1(t_{k+1}) = y_1(t_k) + \dot{y}_1(t_k^+) \Delta_k - \frac{g}{2} \Delta_k^2 \quad (12)$$

$$\dot{y}_1(t_{k+1}^-) = \dot{y}_1(t_k^+) - g \Delta_k \quad (13)$$

$$y_2(t_{k+1}) = y_2(t_k) + \dot{y}_2(t_k^+) \Delta_k + \int_{t_k}^{t_{k+1}} \int_{t_k}^t u(s) ds dt \quad (14)$$

$$\dot{y}_2(t_{k+1}^-) = \dot{y}_2(t_k^+) + \int_{t_k}^{t_{k+1}} u(t) dt \quad (15)$$

$$t_{k+1} = t_k + \Delta_k \quad (16)$$

and then to seek a controller u such that $y_1(t_{k+1}) = y_2(t_{k+1}) = y^*$, $\dot{y}_1(t_{k+1}^+) = \dot{y}_1^*$ and $\dot{y}_2(t_{k+1}^+) = \dot{y}_2^*$ (using also the restitution law). However, it is not easy in general to find such a u . This philosophy has been employed in [5], [6], [7], [35], [36] to control juggling robots. Basically, these authors used the assumption that $\frac{m_1}{m_2} = 0$, i.e., the robot's velocity \dot{y}_2 is not affected by the shocks. Then the open-loop system is reduced to a 2-dimensional system (the ball dynamics in (5)), together with a time-varying unilateral constraint $y_1(t) \geq y_2(t)$. It is then possible to obtain an explicit form of P_Σ . Buehler, *et al.* [5], [6], [7] formulate the problem as designing a feedback control for P_Σ , where the inputs are first considered as being a sequence of flight-times $\Delta_k \triangleq t_{k+1} - t_k$ and robot velocities $\dot{y}_2(t_k^-)$. Then, they propose a heuristic strategy which they call the mirror law (because it aims at making y_1 and y_2 more or less symmetrical with respect to the shock position $y_1 = y_2 = 0$). This work was extended in [22], [23], [24], [25], [26], [27] to more complex jugglers. Experimental results have also been presented by these authors. The control strategies are based on continuous feedback of the object state, measured either *via* cameras [26], [27] or *via* a digitizing table [6], [7]. Vincent [35], [36] directly uses the 2-dimensional map P_Σ derived in [13] and nicely combines results on the bouncing ball dynamics [9] to obtain a hybrid controller. First $y_2(t)$ is set to create chaotic motion of the ball. Then the robot's motion is switched to stabilize (y_1, \dot{y}_1) around a periodic trajectory when its basin of attraction has been attained. The control strategy uses the measurements of flight times obtained *via* a microphone attached to the robot. However, the main drawbacks of this strategy are that the transient period length is not guaranteed, moreover its extension to more complex systems like two dof jugglers is not trivial. Finally, learning techniques have been applied to various juggling systems in [1], [28], [29].

In this work we consider the full dynamics (5)–(8), *i.e.* we allow for discontinuities in \dot{y}_2 . Indeed although the assumption $\frac{m_1}{m_2} = 0$ may be satisfied in some practical cases (like juggling with a ping-pong ball), this is not a universal property, and it may not be satisfied in the general case of pushing-and-striking manipulation tasks. Moreover, its relaxation makes it difficult to employ the above cited strategies, since P_Σ has no longer dimension 2, but 4. Most importantly, let us notice that the design of the force input u in (6) has never been presented in the previous works on the control of juggling robots. We are therefore interested in designing directly the u that is to be implemented on the robot. This note is organized as follows: In section 3 we present the controller and the closed-loop analysis for the one dof juggler. Section 4 is devoted to examine the closed-loop behavior when various types of disturbances (bad knowledge of the restitution coefficient e , bad velocity measurements) are present. Conclusions are given in section 5. Several numerical simulations illustrate the theoretical investigations.

3. Main Results

Before developing the proposed controller u in (6), let us define the objectives of the one dof juggling task: given the dynamics in (5)–(8), make the ball attain a periodic motion from any initial condition $x(0)$, where $x^T = (y_1, y_2, \dot{y}_1, \dot{y}_2)$, and for any $m \triangleq \frac{m_1}{m_2}$ and $e \in [0, 1]$. In other words, since the trajectory $(y_1(t), \dot{y}_1(t))$ can be controlled only through impacts with the robot at times t_k , the goal is to design u in (6) such that the collisions occur at $y_1(t_k) = y_2(t_k) = y_d$, $\dot{y}_1(t_k^+) = \dot{y}_d > 0$, after a possible transient period. Notice that this is equivalent to impose $y_1(t_k) = y_d$ and $t_{k+1} = t_k + \Delta_d$, with $\Delta_d = \frac{2}{g}\dot{y}_d$, or $y_1(t_k) = y_d$ and the trajectory apex $s(k) = s_d = y_d + \frac{\dot{y}_d^2}{2g}$. Nevertheless, as we shall see later, one is also free to choose varying signals $y_d(k)$ and $\dot{y}_d(k)$ to be tracked. Let us note that this definition is slightly different from some other works: for instance in [35], [36], only the apex is regulated while the impact position is not considered. In the next subsection we *a priori* introduce an input u . We shall see further (see remark 5) that it can be deduced from a more general control design methodology.

3.1. The Force Input Controller u

CLAIM 1 *Consider the dynamical system in (5)–(8). Suppose that $x(0)$ and u are such that it exists an impact or a contact time t_0 . Let us define the following control input:*

$$u = m_2 g + m_2 v \tag{17}$$

$$v = A_k(t - t_k) + B_k \tag{18}$$

$k \geq 0$, with

$$A_k = \frac{6}{d_k^2} (\dot{y}_2^*(k+1) + \dot{y}_2(k)) - \frac{12}{d_k^3} (y^*(k+1) - y(k)) \tag{19}$$

$$B_k = -\frac{2}{d_k} (\dot{y}_2^*(k+1) + 2\dot{y}_2(k)) + \frac{6}{d_k^2} (y^*(k+1) - y(k)) \tag{20}$$

$$d_k = \frac{\dot{y}_1(k) + \sqrt{\dot{y}_1^2(k) - 2g(y^*(k+1) - y(k))}}{g} \quad (21)$$

$$\dot{y}_2^*(k+1) = \frac{1+m}{1+e} \dot{y}_1^*(k+1) + \frac{m-e}{1+e} \sqrt{\dot{y}_1^2(k) - 2g(y^*(k+1) - y(k))} \quad (22)$$

where $\dot{y}_1(k) \triangleq \dot{y}_1(t_k^+)$, $\dot{y}_2(k) \triangleq \dot{y}_2(t_k^+)$, $y(k) \triangleq y_1(t_k) = y_2(t_k)$, and $y^*(k+1)$ and $\dot{y}_1^*(k+1)$ are chosen such that

$$y^*(k+1) < h_k \triangleq \begin{cases} y(k) + \frac{\dot{y}_1^2(k)}{2g} & \text{if } \dot{y}_1(k) > 0 \\ y(k) & \text{if } \dot{y}_1(k) \leq 0 \end{cases} \quad (23)$$

and

$$\dot{y}_1(t_k + d_k) - \dot{y}_2^*(k+1) < 0 \quad (24)$$

Then, for all $k \geq 0$:

1. $y_1(t) - y_2(t) > 0, \forall t \in (t_k, t_k + d_k)$
2. $t_{k+1} = t_k + d_k$
3. $y(k+1) = y^*(k+1)$
4. $\dot{y}_1(k+1) = \dot{y}_1^*(k+1)$

Proof: The proof can be found in [40], [39] and is given in appendix A. ■

Remark 2. Controllers as in (52), (53) are basically open-loop. But one notices from (17)–(24) that the controller is computed with $x(t_k^+)$. Consequently u is a state feedback for the system considered as a discrete-time operator at the shock times t_k . More generally, the presented methodology for stabilization of the system in (9)–(11) at some desired trajectory at impact times may be based on a continuous-time feedback of z_2 and a discrete-time feedback of z_1 . This is another common point with the assumptions in [17] (see remark 1).

Remark 3. It clearly appears from (52), (53) that one can modify the matrix F to obtain different controllers in (18) by merely modifying u in (17) (and provided that the obtained system in (6) is controllable with v as the new input). For instance let us choose $u = m_2 g - m_2 \omega_k^2 y_2 + m_2 v$ with $\omega_k = \frac{2\pi}{d_k}$. Then, as shown in [39], [41], the equation $f(y_1(t), y_2(t)) \triangleq y_1(t) - y_2(t) \triangleq f(\Delta)$ can be written as:

$$f(\Delta) = y(k) + \dot{y}_1(k)\Delta - \frac{g}{2}\Delta^2 - \left(y(k) - \frac{A_k}{2\omega_k}\Delta\right)\cos(\omega_k\Delta) - \left(\frac{\dot{y}_2^2(k)}{\omega_k} + \frac{A_k}{2\omega_k^2} + \frac{B_k}{2\omega_k}\Delta\right)\sin(\omega_k\Delta) \quad (25)$$

where $\Delta \triangleq t - t_k > 0$. In order to prove that $f(\Delta) > 0, \forall \Delta \in (0, d_k)$, one must first demonstrate that $f(\Delta)$ has no roots on $(0, d_k)$ which, from (25), is not easy. Since point 1 in claim 1 is crucial for the overall scheme to work, we choose to disregard those controllers for which we cannot prove that it is satisfied. Such conditions of non-existence of “accidental” shocks are general in the analysis of vibro-impact systems. In particular for results concerning existence of periodic trajectories see [12]. They may be called *viability conditions*. They are fundamental conditions in the study of vibro-impact systems which have sometimes been forgotten [20], [30].

Remark 4. Let us define the vector $x_\Sigma(k)^T = (y(k), \dot{y}_1(k), \dot{y}_2(k), t_k)$. Then, the dynamics of the impact Poincaré map

$$P_\Sigma : \quad \Sigma \rightarrow \Sigma$$

$$x_\Sigma(k) \mapsto x_\Sigma(k+1) \quad (26)$$

with $\Sigma = \{(x, t) \in \mathbb{R}^4 \times \mathbb{R}_+ : y_1 - y_2 = 0, \dot{y}_1 - \dot{y}_2 > 0\}$, are guaranteed in closed-loop *via* the chosen input force u in (17)–(24). As we pointed out in the introduction, a possible path for the control design is to use equations (12)–(16). For instance, introducing (17), (18) into (14), (15) one obtains:

$$y_2(k+1) = y_2(k) + \dot{y}_2(k)\Delta_k + \frac{B_k}{2}\Delta_k^2 + \frac{A_k}{6}\Delta_k^3 \quad (27)$$

$$\dot{y}_2(t_{k+1}^-) = \dot{y}_2(k) + B_k\Delta_k + \frac{A_k}{2}\Delta_k^2 \quad (28)$$

Considering (12), (13), (27), (28), (16), and (59), (60), we get a 4-dimensional mapping $x_\Sigma(k+1) = P_\Sigma(x_\Sigma(k), A_k, B_k, \Delta_k)$, given by

$$x_\Sigma(k+1) = \begin{bmatrix} y(k) + \dot{y}_1(k)\Delta_k - \frac{g}{2}\Delta_k^2 \\ \frac{m-e}{1+m}(\dot{y}_1(k) - g\Delta_k) + \frac{1+e}{1+m}\left(\dot{y}_2(k) + \Delta_k B_k + \frac{\Delta_k^2}{2}A_k\right) \\ \frac{m(1+e)}{1+m}(\dot{y}_1(k) - g\Delta_k) + \frac{1-em}{1+m}\left(\dot{y}_2(k) + \Delta_k B_k + \frac{\Delta_k^2}{2}A_k\right) \\ t_k + \Delta_k \end{bmatrix} \quad (29)$$

with A_k, B_k , and Δ_k as control parameters, and an algebraic equation

$$\Delta_k \left[\frac{A_k}{6}\Delta_k^2 + \frac{B_k + g}{2}\Delta_k + (\dot{y}_2(k) - \dot{y}_1(k)) \right] = 0 \quad (30)$$

It is noteworthy that although Δ_k may be considered an input signal for the application in (29), in reality Δ_k is a consequence of the dynamics and of the real input (A_k, B_k) . In fact, from (30), Δ_k can be expressed in terms of A_k and B_k and introduced in (29) to get an explicit system’s Poincaré mapping

$$x_\Sigma(k+1) = \bar{P}_\Sigma(x_\Sigma(k), A_k, B_k) \quad (31)$$

Notice that an expression for Δ_k cannot always be obtained explicitly. Besides, the resultant mapping (31) is usually non-linear in its inputs. This is what renders the design of the control input (A_k, B_k) for tracking purposes directly from (31) a difficult task. One could analyze the stabilization of (31) by linearizing it around a desired trajectory. Then, a local linear feedback can be designed provided the linearization is controllable. Buehler, *et al.* [5], [6], [7] did similarly for their 2-dimensional mapping, but found that such a control strategy does not provide a satisfactory behavior in practice. We have overcome such difficulty using the Dead-beat controllers which allow us to directly assign a value to Δ_k .

Remark 5 (3-step recursive control design). From the above developments it follows that considering the impact Poincaré map \bar{P}_Σ in (31) for control design purposes is not a good solution. As we announced in the introduction of section 3, we now describe a recursive control design method, which will enable us to recover the Dead-beat strategy. Let us define $v(t) = A_k \Delta + B_k$, $\Delta = t - t_k$, with A_k and B_k constants on (t_k, t_{k+1}) . From (12)–(16) and (59) we get

$$\begin{cases} y_1(t_{k+1}) &= y_1(t_k) + \dot{y}_1(t_k^+) \Delta_k - \frac{g}{2} \Delta_k^2 \\ \dot{y}_1(k+1) &= \frac{m-e}{1+m} \dot{y}_1(t_{k+1}^-) + \frac{1+e}{1+m} \dot{y}_2(t_{k+1}^-) \end{cases} \quad (32)$$

and

$$\begin{cases} y_2(t_{k+1}) &= y_2(t_k) + \dot{y}_2(t_k^+) \Delta_k + A_k \frac{\Delta_k^3}{6} + B_k \frac{\Delta_k^2}{2} \\ \dot{y}_2(t_{k+1}^-) &= \dot{y}_2(t_k^+) + A_k \frac{\Delta_k^2}{2} + B_k \Delta_k \end{cases} \quad (33)$$

Step 1: We choose Δ_k and $\dot{y}_2(t_{k+1}^-)$ as the inputs of the system in (32), such that $y_1(t_{k+1}) = y^*(k+1)$, $\dot{y}_1(t_{k+1}^+) = \dot{y}_1^*(k+1)$. This gives

$$\begin{aligned} (32) \Leftrightarrow F_1(x_1(k), x_1^*(k+1), \Delta_k, \dot{y}_2(t_{k+1}^-)) &= 0 \\ &\Rightarrow \begin{cases} \Delta_k = d_k \\ \dot{y}_2(t_{k+1}^-) = \dot{y}_2^*(k+1) \end{cases} \end{aligned} \quad (34)$$

where $x_1^T = (y_1, \dot{y}_1)$; d_k and $\dot{y}_2^*(k+1)$ are given in claim 1 (eqs. (21) and (22) respectively), and for some function F_1 .

Step 2: Introducing the values in (34) into (33), we get $F_2(x(k), d_k, \dot{y}_2^*(k+1), A_k, B_k) = 0$, for some function F_2 , from which we deduce A_k and B_k , which are equal to those in claim 1 (eqs. (19) and (20) respectively).

Step 3: Check viability, i.e., the sign of the function $f(\Delta) \stackrel{\Delta}{=} y_1(t) - y_2(t)$, on (t_k, t_{k+1}) .

It is noteworthy that the success of the first step relies on the ‘‘controllability’’ (or invertibility) properties of the first subsystem with Δ_k and $\dot{y}_2(t_{k+1}^-)$ as inputs. The second step mainly hinges on the satisfaction of the viability conditions. In other words one can choose

another controller structure $v(t)$. For instance

$$v(t) = \sum_{i=0}^n A_{k,i} \Delta^i \quad (35)$$

The viability conditions can be studied from the sign of $f(\Delta)$ as in (57), which is a polynomial in Δ . Clearly for $n \geq 2$ in (35), the sign of $f(\Delta)$ is not easy to obtain. This is why the solution $n = 1$ has been chosen. Let us finally notice that it is not proven yet that to each (polynomial) controller as in (35) there corresponds a Dead-beat controller (possibly designed after a dynamic pre-feedback in order to get the right matrix F in (51)–(53)). Extending the above procedure to systems as in (9)–(11) is a topic of future research.

3.2. Definition of the Desired Trajectories

The next step is to define the signals $y^*(k+1)$ and $\dot{y}_1^*(k+1)$ which can be regarded as the desired trajectory of the ball. We still consider the system at a generic impact time t_k .

COROLLARY 1 *Let $y^*(k+1)$ and $\dot{y}_1^*(k+1)$ be given as:*

$$y^*(k+1) = \begin{cases} y_d & \text{if } h_k > y_d \\ y(k) + r & \text{if } h_k \leq y_d \end{cases} \quad (36)$$

$$\dot{y}_1^*(k+1) = \begin{cases} \dot{y}_d & \text{if } h_k > y_d \\ \sqrt{\dot{y}_d^2 + 2g(y_d - y(k) - r)} & \text{if } h_k \leq y_d \end{cases} \quad (37)$$

where $\dot{y}_d > 0$, and r is a real value chosen such that condition (23) is satisfied, i.e., $y(k) + r < h_k$. Then (x_k, Δ_k) converges towards its desired value $(x_d, \Delta_d) = (y_d, y_d, \dot{y}_d, \frac{1-e-2em}{1+e}\dot{y}_d, \frac{2}{g}\dot{y}_d)$ after at most 2 impacts, i.e., $(x_{k+i}, \Delta_{k+i}) = (x_d, \Delta_d) \forall i \geq j \in \{0, 1, 2\}$.

Proof: From claim 1 and (29), it is easy to verify that whenever the control input (17)–(24) is applied, the system's impact Poincaré mapping (26) is given by

$$x_\Sigma(k+1) = \begin{bmatrix} y^*(k+1) \\ \dot{y}_1^*(k+1) \\ \frac{1-em}{1+e}\dot{y}_1^*(k+1) - \frac{e(1+m)}{1+e}\sqrt{\dot{y}_1^2(k) - 2g(y^*(k+1) - y(k))} \\ t_k + \frac{\dot{y}_1(k) + \sqrt{\dot{y}_1^2(k) - 2g(y^*(k+1) - y(k))}}{g} \end{bmatrix} \quad (38)$$

From the iterative substitution of (36) and (37) in (38), the proof follows. ■

Notice that this constitutes mainly a theoretical result, since in practice more than two shocks will often be necessary before the convergence to the desired value, mainly due to input saturations. In the next subsection a strategy is proposed to cope with this problem.

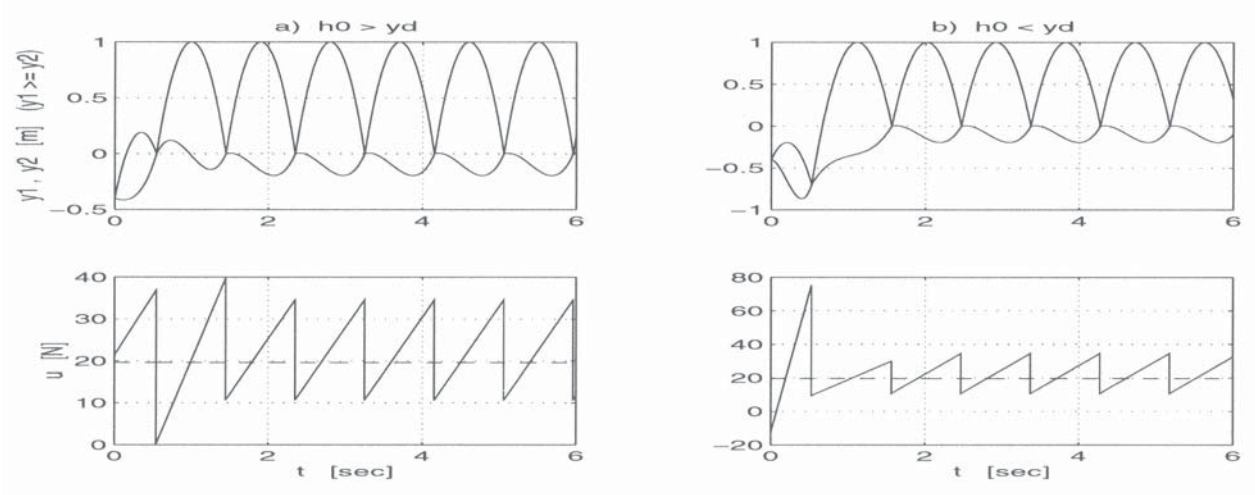


Figure 2. Results of example 1: a) $h_0 > y_d$; b) $h_0 \leq y_d$.

Example 1. Let us consider the application of the control strategy (17)–(22), (36) and (37) to a one dof juggler with $e = 0.7$, $m_1 = 0.3$ kg, $m_2 = 2$ kg (which gives $m = 0.15$), $y_d = 0$, $\dot{y}_d = 4.43$ m/s (which is equivalent to $s_d = 1$ m), $y(0) = -0.4$ m, $\dot{y}_2(0) = -0.2$ m/s. In figure 2, one can observe the trajectories followed by the ball and the surface in the upper graphs and the control input force in the lower ones (where the dashed line indicates the surface weight, $m_2g = 19.62$ N). Two cases are considered: a) $\dot{y}_1(0) = 3.4$ m/s which gives $h_0 = 0.2$ m > 0 , and b) $\dot{y}_1(0) = 2$ m/s which gives $h_0 = -0.2$ m < 0 . This shows the two possible initial cases: $h_0 > y_d$ and $h_0 \leq y_d$ respectively.

3.3. Control Magnitude Reduction via Desired Motion Modification

The impact trajectories defined in (36) and (37) are designed in such a way that the ball reaches the desired apex $s_d = y_d + \frac{\dot{y}_d^2}{2g}$ just after the first control collision. This may require continuous-time input forces of big magnitudes during the first flight interval ($t_0, t_0 + d_0$) (see figure 2b). Let us consider the realistic case where the final actuator of the juggling robot provides forces bounded in magnitude such that $|u| \leq u_{max}$. From (18), this implies $v_1 \leq v \leq v_2$. One sees from (36) and (37) that the signals $y^*(k+1)$ and $\dot{y}_1^*(k+1)$ can be chosen time-varying in order to cope with the input magnitude. Intuitively, one easily conceives that the desired apex s_d can be attained by imparting several small strikes to the ball rather than one big hit (this is for instance what one does with a racket to make a tennis ball rebound higher and higher). In this subsection we present such a strategy.

COROLLARY 2 *Let us consider that $v_1 < \frac{-3+e-2m+2em}{1+e}g$ and $v_2 > \frac{3-2e+4m-em}{1+e}g$, and assume that:*

1. *The impact states just after the first shock at t_0 are such that $\dot{y}_1(0) > 0$ and*

$$-\frac{v_2}{g}\dot{y}_1(0) \leq \dot{y}_2(0) \leq \min\{M_1, M_2, 1\}\dot{y}_1(0)$$

where $M_1 = -\frac{1}{2} \left(\frac{v_1}{g} + \frac{m-e}{1+e} + \frac{e}{M_3} \frac{1+m}{1+e} \right)$, $M_2 = \frac{v_2}{g} - \frac{2(m-e)}{1+e} - \frac{2e}{M_3} \frac{1+m}{1+e}$, $M_3 = \min\{M_4, M_5\}$, $M_4 = \frac{1+e}{1+m} \frac{v_2}{2g} + \frac{3-e+2m-2em}{2(1+m)}$, and $M_5 = -\frac{1+e}{1+m} \frac{v_1}{g} + \frac{3-2e+4m-em}{1+m}$.

2. The desired trajectories are designed, at each impact, as: $y^*(k+1) = y(k)$ and

$$\dot{y}_1^*(k+1) = \begin{cases} N_1(k) & \text{if } \dot{y}_d < N_1(k) \\ \dot{y}_d & \text{if } N_1(k) \leq \dot{y}_d \leq N_2(k) \\ N_2(k) & \text{if } \dot{y}_d > N_2(k) \end{cases} \quad (39)$$

$\forall k \geq 0$, for any positive value of \dot{y}_d , where $N_1(k) = \max \left\{ N_3(k), N_4(k), \frac{e}{M_3} \dot{y}_1(k) \right\}$, $N_2(k) = \min \{N_5(k), N_6(k)\}$, $N_3(k) = -\left(\frac{1+e}{1+m} \frac{v_2}{g} + \frac{m-e}{1+m} \right) \dot{y}_1(k) - \frac{2(1+e)}{1+m} \dot{y}_2(k)$, $N_4(k) = \left(\frac{1+e}{1+m} \frac{v_1}{2g} - \frac{m-e}{1+m} \right) \dot{y}_1(k) - \frac{1+e}{2(1+m)} \dot{y}_2(k)$, $N_5(k) = -\left(\frac{1+e}{1+m} \frac{v_1}{g} + \frac{m-e}{1+m} \right) \dot{y}_1(k) - \frac{2(1+e)}{1+m} \dot{y}_2(k)$, and $N_6(k) = \left(\frac{1+e}{1+m} \frac{v_2}{2g} - \frac{m-e}{1+m} \right) \dot{y}_1(k) - \frac{1+e}{2(1+m)} \dot{y}_2(k)$.

Then, the impact velocity of the ball converges to \dot{y}_d without saturating the input, i.e., $v_1 < v(t) < v_2$, $\forall t \geq t_0$.

Proof: The proof can be found in [39], [40] and is not given in this note for the sake of brevity. ■

Let us explain the underlying philosophy of the strategy presented in corollary 2. Assume that v_1 and v_2 are as pointed out in the corollary, and that an impact such that $\dot{y}_1(k) > 0$ takes place. Let us define the desired impact position as $y^*(k+1) = y(k)$. Then, in order to have $\dot{y}_1(k+1) > 0$ without saturating the control input, $\dot{y}_2(k)$ must be within

$$\Omega_1(k) \triangleq \left\{ \dot{y}_2(k) \in \mathbb{R} : -\frac{v_2}{g} \dot{y}_1(k) \leq \dot{y}_2(k) \leq \min(M_1, M_2, 1) \dot{y}_1(k) \right\}$$

(M_1 and M_2 are defined in point 1 of corollary 2), and the set of nonnegative values within which $\dot{y}_1^*(k+1)$ must be selected is

$$\Omega_2(k) \triangleq \{ \dot{y}_1^*(k+1) \in \mathbb{R} : N_1(k) \leq \dot{y}_1^*(k+1) \leq N_2(k) \}$$

($N_1(k)$ and $N_2(k)$ are defined in point 2 of corollary 2). Besides, in order for $\Omega_2(k)$ to include $\dot{y}_1(k)$, so that $\dot{y}_1^*(k+1)$ can be chosen greater or smaller than, or even equal to, $\dot{y}_1(k)$ (having all these possibilities in the same time), $\dot{y}_2(k)$ must be within

$$\Omega_3(k) \triangleq \{ \dot{y}_2(k) \in \mathbb{R} : \max(P_1, P_2) \dot{y}_1(k) \leq \dot{y}_2(k) \leq \min(P_3, P_4, 1) \dot{y}_1(k) \} \subset \Omega_1(k)$$

where $P_1 = \frac{v_1}{g} - \frac{2(1-e+2m)}{1+e}$, $P_2 = -\frac{1}{2} \left(\frac{v_2}{g} + \frac{1-e+2m}{1+e} \right)$, $P_3 = -\frac{1}{2} \left(\frac{v_1}{g} + \frac{1-e+2m}{1+e} \right)$, and $P_4 = \frac{v_2}{g} - \frac{2(1-e+2m)}{1+e}$. Moreover, the selection of $\dot{y}_1^*(k+1) \in \Omega_2(k)$ ensures that $\dot{y}_2(k+1)$ will be within $\Omega_3(k+1)$, for any $\dot{y}_2(k) \in \Omega_1(k)$. Now, notice that the conditions established in

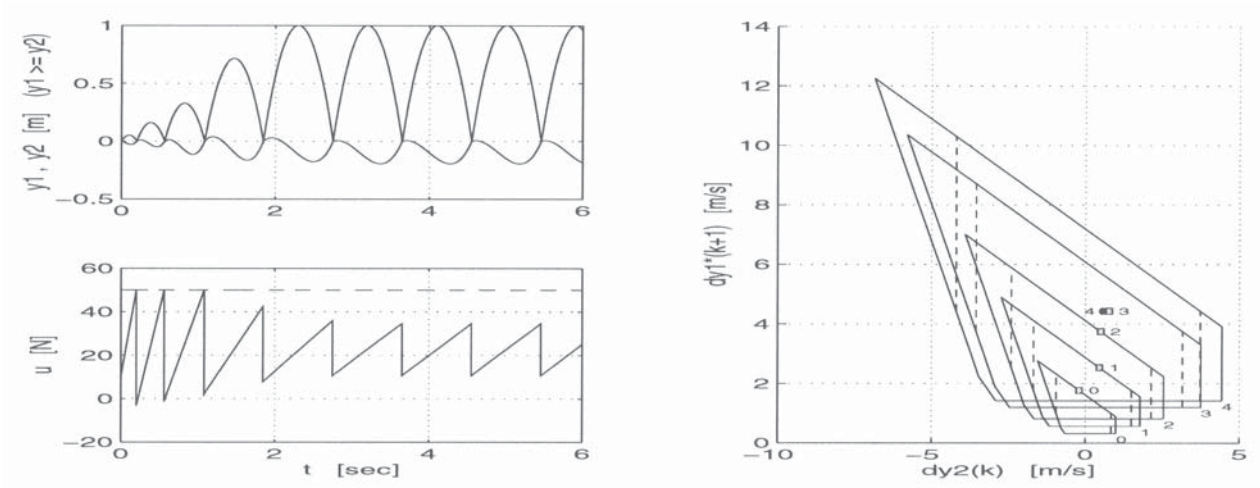


Figure 3. Bounded input force strategy.

point 1 and the design criterion proposed in point 2 of corollary 2 are such that $\dot{y}_2(0) \in \Omega_1(0)$ and $\dot{y}_1^*(k+1) \in \Omega_2(k)$, $\forall k \geq 0$. Moreover, (39) always assigns to $\dot{y}_1^*(k+1)$ the closest value to $\dot{y}_d > 0$ inside $\Omega_2(k)$. Then, the convergence of $\dot{y}_1(k)$ to \dot{y}_d and the non-saturation of the input are guaranteed simultaneously. This criterion is repeated at each impact until a collision such that $\dot{y}_d \in \Omega_2(k)$ takes place. From this moment, according to (39), the desired value is selected, *i.e.* $\dot{y}_1^*(k+1) = \dot{y}_d$. Notice that the subsets $\Omega_i(k)$, $i = 1, 2, 3$, need not be calculated. Just the value of $N_1(k)$ or $N_2(k)$ in (39) must be computed at each impact.

Example 2. Let us consider the same juggler and the same desired trajectory as in the previous example, but with initial impact conditions given by $y(0) = 0$, $\dot{y}_1(0) = 1$ m/s, and $\dot{y}_2(0) = -0.2$ m/s. Assume, this time, that the force is bounded such that $|u| \leq 50$ N. In the left-hand side of figure 3, one can see the result of the application of the strategy in corollary 2 (the dashed line indicates the force limit $u_{max} = 50$ N). Observe that the ball approaches progressively the desired motion, and that the force remains always within its limits. In the right-hand side of figure 3, one can see the evolution of the subspaces $\bar{\Omega}_1(k) \triangleq \Omega_1(k) \times \Omega_2(k)$ (bounded by full lines) and $\bar{\Omega}_2(k) \triangleq \Omega_3(k) \times \Omega_2(k)$ (bounded by full and dashed lines). The squares represent the values of $\dot{y}_1^*(k+1)$ chosen at every collision (according to $\dot{y}_2(k)$). The dark dot represents \dot{y}_d . The digits stand for the impact number k . Notice that $\dot{y}_2(k) \in \Omega_3(k)$, $\forall k \geq 1$.

Figure 3 shows that the application of the foregoing algorithm not only helps maintaining the force within certain limits but also keeps the robot trajectory with small amplitudes. A numerical study showed that, in general, increasing the number of impacts during the transient reduces the limits within which y_2 evolves. In figure 4, the maximum and minimum values of y_2 at each flight time (corresponding to $\dot{y}_2 = 0$) are plotted *versus* time for the same juggler in example 2, with initial collision velocities given by $\dot{y}_1(0) = 0.5$ m/s $<$ $\dot{y}_d = 4.43$ m/s and $\dot{y}_2(0) = -0.7$ m/s. The bounded input algorithm was applied four times, each time increasing the number of collisions during the transient. The different

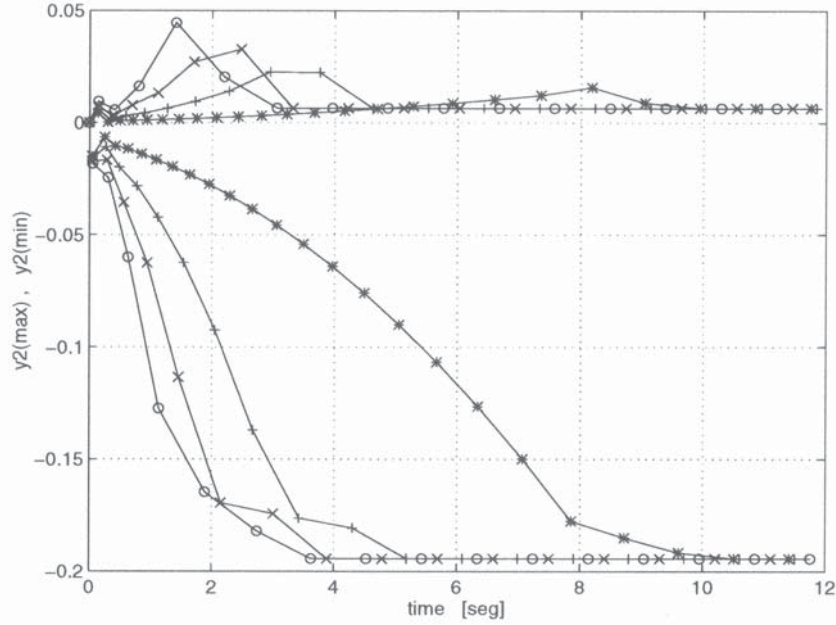


Figure 4. Decreasing the robot trajectory amplitudes.

cases were marked, in increasing order of transient shocks, by \circ , \times , $+$, $*$. Notice that the number of impacts in which the desired motion is reached is not predefined by the bounded input control algorithm (or by the designer). However, this one ensures as least as possible transient collisions since (39) assigns to $\dot{y}_1^*(k+1)$ the closest value to \dot{y}_d inside $\Omega_2(k)$ at each impact. Hence, in order to increase the number of transient shocks, the following criterion was established: A coefficient $\beta < 1$ was defined (recall that $\dot{y}_1(0) < \dot{y}_d$). Then, at each collision, if $N_2(k) \neq \dot{y}_d$, the actual value of $\dot{y}_1^*(k+1)$ used by the control law was β times the value chosen by the algorithm, *i.e.* $\dot{y}_1^*(k+1) = \beta N_2(k)$. Since smaller values of $\dot{y}_1^*(k+1)$ are used, more transient shocks take place. The coefficients used to obtain figure 4 were $\beta_\circ = 1$, $\beta_\times = 0.9$, $\beta_+ = 0.8$, and $\beta_* = 0.7$. Observe that increasing the number of transient impacts causes y_2 to remain within a smaller interval. This strategy can be used to keep not only u but also y_2 between two bounds.

Finally, let us notice that we could have defined $\dot{y}_2(0) \in \Omega_3(0)$ as initial condition in point 1 of corollary 2 (instead of $\dot{y}_2(0) \in \Omega_1(0)$). This would have ensured sequences of the ball impact velocity of the form: $\{\dot{y}_1(k) : 0 < \dot{y}_1(0) < \dot{y}_1(1) < \dot{y}_1(2) < \dots < \dot{y}_d\}$ if $\dot{y}_1(0) < \dot{y}_d$, $\{\dot{y}_1(k) : \dot{y}_1(0) > \dot{y}_1(1) > \dot{y}_1(2) > \dots > \dot{y}_d > 0\}$ if $\dot{y}_1(0) > \dot{y}_d$, or $\{\dot{y}_1(k) : \dot{y}_1(k) = \dot{y}_d > 0, \forall k \geq 0\}$ if $\dot{y}_1(0) = \dot{y}_d$. Nevertheless, $\dot{y}_2(0) \in \Omega_3(0)$ is a more restrictive condition compared with $\dot{y}_2(0) \in \Omega_1(0)$ since $\Omega_3(0) \subset \Omega_1(0)$. That is why $\dot{y}_2(0)$ is permitted to be within $\Omega_1(0)$ rather than within $\Omega_3(0)$. In any case, recall that the design criterion in point 2 of corollary 2 ensures $\dot{y}_2(k) \in \Omega_3(k)$ for all $k \geq 1$ and the selection of $\dot{y}_1^*(k+1) > 0$ (always positive) for all $k \geq 0$. The difference is that if at impact 0 the shock velocities are such that: $\min\{P_3, P_4\}\dot{y}_1(0) < \dot{y}_2(0) \leq \min\{M_1, M_2, 1\}\dot{y}_1(0)$ and $\dot{y}_1(0) \leq \dot{y}_d$, then the sequence of ball impact velocities is of the form $\{\dot{y}_1(k) : \dot{y}_1(0) > \dot{y}_1(1) > 0, \dot{y}_1(1) < \dot{y}_1(2) < \dots < \dot{y}_d\}$; or if: $-\frac{v_2}{g} \leq \dot{y}_2(0) < \min\{P_1, P_2\}\dot{y}_1(0)$ and $\dot{y}_1(0) \geq \dot{y}_d$, then $\{\dot{y}_1(k)\}$ has the form $\{\dot{y}_1(k) : 0 < \dot{y}_1(0) < \dot{y}_1(1) > \dot{y}_1(2) > \dots > \dot{y}_d > 0\}$. Notice

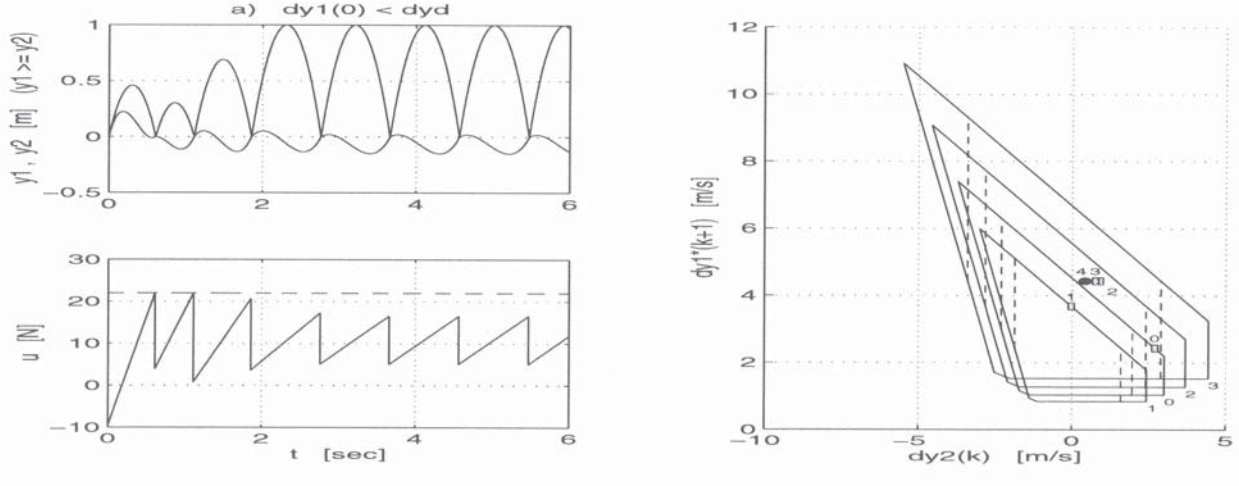


Figure 5. Bounded input strategy: $\{\dot{y}_1(k) : \dot{y}_1(0) > \dot{y}_1(1) > 0, \dot{y}_1(1) < \dot{y}_1(2) < \dots < \dot{y}_d\}$.

that even if $\dot{y}_1(0) = \dot{y}_d$, the sequence must first go away from its goal, \dot{y}_d , and come back to it later. An illustration of this phenomenon is given in figure 5 for a juggler with $m_1 = 0.1$ kg, $m_2 = 1$ kg (then $m = 0.1$), $\dot{y}_d = 4.43$ m/s, $y(0) = 0$, $\dot{y}_1(0) = 3$ m/s $< \dot{y}_d$, $\dot{y}_2(0) = -4.5$ m/s, and $u_{max} = 22$ N.

3.4. Relationship with Buehler-Koditschek's Mapping and Mirror Law

As recalled in [40], [42] the studies in [5], [6], [7] essentially focused on the derivation of a one-dimensional non-linear mapping for the ball velocity. However, only a heuristic control strategy (mirror law) has been proposed in [5], [6], [7]. In this section we show how their results may be used in the framework of the hybrid strategy proposed in (17)–(22), (36) and (37). We also emphasize the relationships between their mirror law and our algorithm.

As we previously pointed out, the signals $y^*(k+1)$ and $\dot{y}_1^*(k+1)$ in (19)–(24) can be chosen differently. For instance, let us consider that (36) holds, but that we choose $\dot{y}_1^*(k+1)$ as

$$\dot{y}_1^*(k+1) = \begin{cases} h_1(w_1(k)) & \text{if } h_k > y_d \\ h_2 \circ h_1(w_2(k)) & \text{if } h_k \leq y_d \end{cases} \quad (40)$$

where $h_1(w) = [1 + \gamma (\dot{y}_d^2 - w^2)] w$, $h_2(w) = \sqrt{w^2 + 2g(y_d - y(k) - r)}$, $w_1(k) = \sqrt{\dot{y}_1^2(k) - 2g(y_d - y(k))}$, $w_2(k) = \sqrt{\dot{y}_1^2(k) - 2gr}$, and $0 < \gamma < \frac{1}{\dot{y}_d^2}$. Then, after at most two collisions, the ball impact states will be given by $y(k+1) = y(k) = y_d$ and

$$\dot{y}_1(k+1) = [1 + \gamma (\dot{y}_d^2 - \dot{y}_1^2(k))] \dot{y}_1(k) \quad (41)$$

Buehler, *et al.* [5], [6], [7] proposed a different way (the mirror law) to make the ball impact velocity follow the behavior stated by mapping (41) for a specific case of the one dof juggler ($m = 0$, $y_d = 0$), and showed that (41) is asymptotically stable [5, p. 72]. Let us now

suppose that $\dot{y}_1^*(k+1)$ is as in (40) and that $m > 0$, but that the scheme is designed with the assumption $m = 0$, as done in [7], [6], [5]. Then from (22) (with $m = 0$) and (59), one obtains

$$\dot{y}_1(k+1) = \left[\frac{1-m}{1+m} + \frac{\gamma}{1+m} (\dot{y}_d^2 - \dot{y}_1^2(k)) \right] \dot{y}_1(k) \quad (42)$$

$\forall k \geq i \in \{0, 1, 2\}$. It follows that the fixed point (y_d, \dot{y}_d) is modified to the one of the mapping in (42), i.e., $(y_d, \sqrt{\dot{y}_d^2 - \frac{2m}{\gamma}})$. Although the mapping in (42) is always stable for a choice of $\gamma \in (0, \frac{1}{\dot{y}_d^2})$ [5, p. 72] and for all $m \in [0, 1)$ such that the fixed point of the real mapping exists (i.e., $\dot{y}_d^2 - \frac{2m}{\gamma} > 0$), the assumption $m = 0$ may introduce convergence problems and significant tracking errors on the desired velocity and apex if in reality $m > 0$.

Now, as shown previously, the formulation of the robotic juggling problem is divided in two phases: the design of the continuous-time input force and the definition of the impact trajectories. Buehler, *et al.* [5], [6], [7] proposed a continuous-time surface trajectory consisting of a mirror-like ‘‘reflex’’ of the ball’s trajectory with a ‘‘distortion’’ gain (α_k) that changes every flight-time in such a way that (41) takes place, i.e.,

$$y_2 = -\alpha_k y_1 \quad (43)$$

where $\alpha_k = \frac{1-e}{1+e} + \frac{\gamma}{1+e} [\dot{y}_d^2 - \dot{y}_1^2(k)]$. The controller given by (17)–(22), (36) and (37) follows a similar behavior, but the ball’s trajectory is rather reflected by the surface velocity. Indeed from (13), it is not difficult to realize that (18) can be written as $v = -\frac{A_k}{g} \dot{y}_1(t) + C_k$, where $C_k = \frac{\dot{y}_1(k)}{g} A_k + B_k$. After integrating the surface dynamics, one gets

$$\dot{y}_2(t) = -\frac{A_k}{g} y_1(t) + D_k + C_k (t - t_k) \quad (44)$$

where $D_k = \dot{y}_2(k) + \frac{y(k)}{g} A_k$. Considering the desired trajectories (36) and (37), one realizes that after at most two impacts, the last term in the right-hand side of (44) becomes dependent just on m . This means that it helps the surface to recover from the perturbations due to impacts. If $m = 0$, it disappears. The second term is an offset that helps the surface to adjust the impact positions and velocities to the desired ones. If it did not exist and, for example, the desired impact position were zero, the surface collision speed would also be zero which would not make any sense for the generic case $e \in [0, 1)$. Actually, choosing (43) constrained Buehler, *et al.* to define the origin as the only possible desired impact position, while (44) permits the definition of any value for y_d or even a sequence of values. Finally, the first term expresses the mirror-like reflex of the ball’s trajectory by the surface velocity.

4. Robustness Analysis

The class of feedback controllers derived in the foregoing section relies on three essential facts: First, it is supposed that the object’s postimpact velocities $\dot{y}_1(k)$ are exactly known.

Second, we assume that there is no disturbance on the ball during the flight-times, so that its motion is perfectly known. Third, the system's parameters are well-known. In practice, it may happen that one or several of these assumptions are not satisfied. Let us consider the following cases: *i*) $\dot{y}_1(k)$ and the ball's motion are well-known but the coefficient e is estimated by $\hat{e} \neq e$. Then the signal $\dot{y}_2^*(k+1)$ in (22) will be different from the ideal one, but the collisions will occur at the desired position and at $t_{k+1} = t_k + d_k$. *ii*) $\dot{y}_1(k)$ or the ball's motion or both are not well-known. Then the collision will not in general occur at the desired height and $t_{k+1} \neq t_k + d_k$. The main discrepancy between these two situations is that in the first case, the dynamics on the impact Poincaré section is known. Whereas in the second case, we will have to derive the expression of the impact Poincaré map P_Σ as a result of the closed-loop dynamics with disturbances. In other words the control law will no longer guarantee the location of the impacts (hence of the section Σ). In general the impact Poincaré map will be impossible to calculate explicitly.

4.1. Unknown Restitution Coefficient

Let us suppose that we compute (17)–(22) using an estimate of the restitution coefficient \hat{e} which value is different from the real e , i.e., $\hat{e} \neq e$, but we still assume that the postimpact velocities are measured correctly. Then, after integrating the dynamics (5), (6) considering (17)–(24), it is easy to realize that the next impact position does not change, i.e., $y_1(k+1) = y_2(k+1) = y^*(k+1)$. Moreover, the velocity of the surface just before the next impact will be the calculated one, i.e., $\dot{y}_2(t_{k+1}^-) = \dot{y}_2^*(k+1)$, which we would compute as (see (22))

$$\dot{y}_2^*(k+1) = \frac{1+m}{1+\hat{e}} \dot{y}_1^*(k+1) + \frac{m-\hat{e}}{1+\hat{e}} \sqrt{\dot{y}_1^2(k) - 2g(y^*(k+1) - y(k))} \quad (45)$$

On the contrary, the system's impact velocities are the states that are affected by this discrepancy ($\hat{e} \neq e$). Indeed, let us analyze the behavior of the ball impact velocities. From (59), (45), and the integrated dynamics of the ball (12), (13), one obtains

$$\dot{y}_1(k+1) = \frac{1+e}{1+\hat{e}} \dot{y}_1^*(k+1) + \frac{e-\hat{e}}{1+\hat{e}} \sqrt{\dot{y}_1^2(k) - 2g(y^*(k+1) - y(k))} \quad (46)$$

Let us for the moment consider the case in which $h_k > y_d$. Then, from (36), (37) in (46), we get

$$\dot{y}_1(k+1) = \frac{1+e}{1+\hat{e}} \dot{y}_d + \frac{e-\hat{e}}{1+\hat{e}} \sqrt{\dot{y}_1^2(k) - 2g(y_d - y(k))} \quad (47)$$

Assuming that the difference $e - \hat{e}$ is such that $h_{k+j} > y_d, \forall j \geq 1$, we have for all $j \geq 2$

$$\dot{y}_1(k+j) = \frac{1+e}{1+\hat{e}} \dot{y}_d + \frac{e-\hat{e}}{1+\hat{e}} \dot{y}_1(k+j-1)$$

Then by induction, one can verify that

$$\dot{y}_1(k+j) = \left[1 - \left(\frac{e-\hat{e}}{1+\hat{e}} \right)^j \right] \dot{y}_s + \left(\frac{e-\hat{e}}{1+\hat{e}} \right)^j \sqrt{\dot{y}_1^2(k) - 2g(y_d - y(k))} \quad (48)$$

for all $j \geq 1$, where $\dot{y}_s = \frac{1+e}{1+2\hat{e}-e} \dot{y}_d$. In the same way, for the case in which $h_k \leq y_d$, we get for all $j \geq 2$

$$\dot{y}_1(k+j) = \left[1 - \left(\frac{e-\hat{e}}{1+\hat{e}} \right)^{j-1} \right] \dot{y}_s + \left(\frac{e-\hat{e}}{1+\hat{e}} \right)^{j-1} \sqrt{\dot{y}_1^2(k+1) - 2g(y_d - y(k) - r)} \quad (49)$$

It is easy to verify that $\left| \frac{e-\hat{e}}{1+\hat{e}} \right| < 1$, $\forall (e, \hat{e}) \in [0, 1] \times [0, 1] : (e, \hat{e}) \neq (1, 0)$ ⁽²⁾. From (48) and (49), one realizes that whatever the relationship between h_k and y_d is, the impact velocity of the ball converges to \dot{y}_s , i.e., $\lim_{j \rightarrow \infty} \dot{y}_1(k+j) = \dot{y}_s$. Following the same analysis for the impact velocity of the surface, we find that the system's collision states converge to $x_s = (y_d, y_d, \dot{y}_s, \frac{1-e-2em}{1+2\hat{e}-e} \dot{y}_d)$. It is noteworthy that the convergence is ensured assuming that $h_{k+j} > y_d, \forall j \geq 1$. From a detailed analysis, one can realize that a sufficient condition for this to be true is the subestimation of the restitution coefficient, i.e., $\hat{e} < e$. Indeed, let us again consider the case in which $h_k > y_d$. Since $y(k+1) = y^*(k+1)$, from (36) $y(k+1) = y_d$. Hence, $\dot{y}_1(k+1)$ must be positive for $h_{k+1} > y_d$ to be satisfied. From (47), it is easy to see that if $e - \hat{e} > 0$ then $\dot{y}_1(k+1) > 0$. Continuing this analysis for $j \geq 2$, one realizes from (48) that if $e - \hat{e} > 0$ then $\dot{y}_1(k+j) > 0, \forall j \geq 2$, and hence $h_{k+j} > y_d, \forall j \geq 1$. For the case in which $h_k \leq y_d$, if $h_{k+1} > y_d$ then it is easy to verify that the same analysis can be made for $j \geq 2$ (see (49)) and that it leads to the same result. It can also be proved that for $h_{k+1} > y_d$ to be true, $e > \hat{e}$ is also a sufficient condition. Finally, for the case in which $\hat{e} > e$, a small enough difference $\hat{e} - e$ is desirable.

4.2. Errors in the Ball's Velocity Measurements

In order to show what happens when the impact velocities of the ball are not well measured, let us consider the same one dof juggler of Example 1, with the same desired trajectory (y_d, \dot{y}_d) (and initial conditions of case a). Several simulations were executed introducing a noise signal to the measured impact speed according to the following expression: $\hat{v}_1(k) = (1 - \alpha + 2\alpha\rho)\dot{y}_1(k)$, where $\hat{v}_1(k)$ is the measured collision velocity, ρ is a random signal with values in $[0, 1]$, and $\alpha \in [0, 1]$ is an indicator of the noise level, such that $\hat{v}_1(k)$ is randomly within $[(1 - \alpha)\dot{y}_1(k), (1 + \alpha)\dot{y}_1(k)]$, for all $k \geq 0$. α was varied from 0 to 0.2 every 0.01 units. Each simulation includes around 30 impacts and they were repeated 10 times for each noise level. An average radius $\|x(k) - x_d\|_2$ was obtained for each simulation. The result is shown in figure 6. We conclude that the error distance is in general bounded and proportional to the noise level (despite the existent dispersion). The impact states remain in a neighborhood around the desired fixed point and a destabilisation of the closed-loop system does not in general occur.

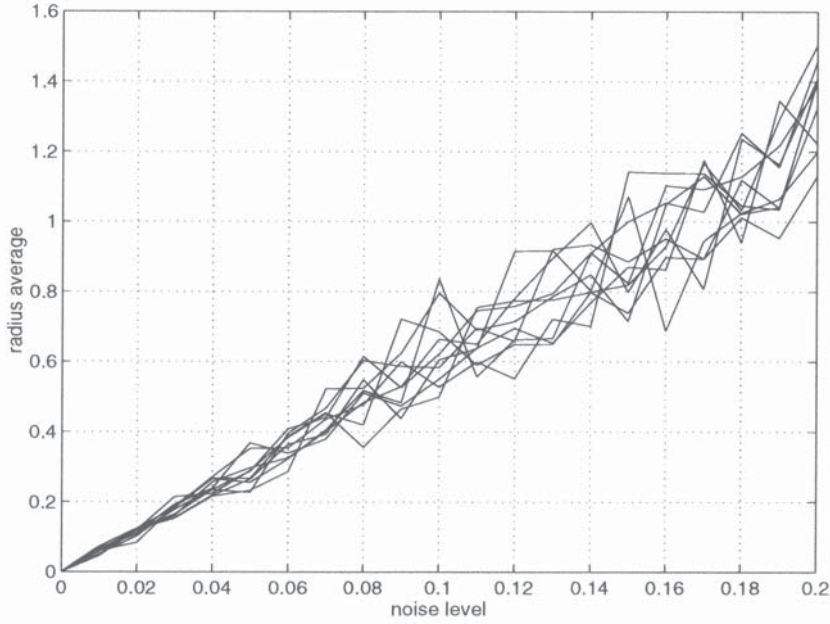


Figure 6. Average of $\|x(k) - x_d\|_2$ for different noise levels.

4.3. Computed Impact Velocities and Restitution Coefficient Estimation

In practice, it is difficult to have exact impact velocity measurements and they are usually noisy [5], [7]. On the contrary, detecting the positions where the ball's velocity is zero (apex) $s(k)$ is in general much easier. From this and the fact that the free-motion and impact dynamics are well-known, we propose a noiseless method for the knowledge of the ball's velocities (we suppose that the rest of the impact states are exactly measurable). It consists of the computation of this impact state using apex measurements. Indeed, from (59) we get an expression for the calculation of $\dot{y}_1(k+1)$ given by

$$\dot{y}_1(k+1) = \frac{m - \hat{e}}{1 + m} \dot{y}_1(t_{k+1}^-) + \frac{1 + \hat{e}}{1 + m} \dot{y}_2(t_{k+1}^-)$$

where we have replaced the real Newton restitution coefficient e by an estimation \hat{e} . The term $\dot{y}_1(t_{k+1}^-)$ can be calculated from the free-motion dynamics of the ball, the desired impact trajectories and the knowledge of $s(k)$. A disadvantage of this method is the possibility of having $\hat{e} \neq e$. This case is analyzed *via* simulation for the juggler previously described in Example 1, with the same desired trajectory (y_d, \dot{y}_d) (and initial conditions of case a). Figure 7 shows the results obtained for: a) $(e, \hat{e}) = (0.7, 0.5)$, and b) $(e, \hat{e}) = (0.7, 0.9)$. We can observe that a periodic motion is always attained, i.e., $\lim_{k \rightarrow \infty} x(k) = x_s$. For the case $\hat{e} > e$, the ball impact states are characterized by $y_s < y_d$ and $\dot{y}_s < \dot{y}_d$. On the contrary, when $\hat{e} < e$, it can be seen that $y_s > y_d$ and $\dot{y}_s > \dot{y}_d$. As expected, an underestimation of e makes the robot hit the ball with a too large velocity. An overestimation implies the opposite effect. Notice (compare figures 7 and 2) that an error of 30% on e results in an error of 500% of the apex for the underestimation (remember that the desired apex was

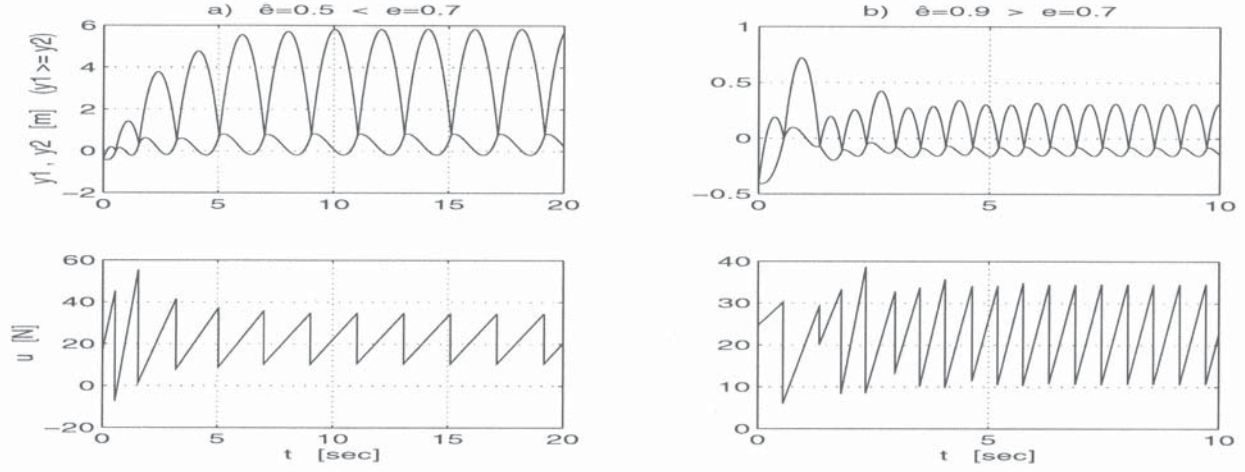


Figure 7. Computed impact velocities: a) $\hat{e} < e$; b) $\hat{e} > e$.

defined above as $s_d = 1$ m) and 70% for the overestimation. One therefore concludes that the accurate knowledge of e is very important.

In order for the impact states to attain asymptotically the desired fixed point (x_d, Δ_d) , a heuristic adaptive law was implemented for \hat{e} in terms of the apex error: $\hat{e}(k+1) = \hat{e}(k) + a \left(\frac{s(k) - s_d}{s_d} \right)$, where $a \in \mathbb{R}$ is the adaption gain. Figure 8 shows (considering the same juggler as above) the evolution of the errors $y(k) - y_d$, $s(k) - s_d$, and $\hat{e}(k) - e$, for $a = 0.025$, $e = 0.7$ and: a) $\hat{e}(0) = 0.5$, and b) $\hat{e}(0) = 0.9$. These and several other numerical results have shown that for $|\hat{e}(0) - e|$ and an adaption gain a both small enough, convergence of $(x(k), \hat{e}(k)) \rightarrow (x_d, e)$ occurs.

Object dynamics with damping. Finally, the robustness of the control scheme with respect to unknown damping acting on the object during the flight times has been studied in [39], [40]. Since the impact Poincaré map is impossible to obtain explicitly in that case, numerical simulations have been presented. They show that for small enough (but strictly larger than zero) damping and the same desired trajectories as in example 1, the ball closed-loop trajectories still converge towards a periodic motion with one impact *per* period.

5. Conclusions

A family of feedback controllers is presented for one degree-of-freedom juggling robots. Due to the potential applications of such study in non-prehensile manipulation, in which the mass of the object is not necessarily negligible with respect to that of the robot, a 4-dimensional model of the system has been considered. The hybrid control strategy mainly consists of a discrete-time state feedback. It is flexible enough to cope with various juggling tasks and can be designed so that the impact position and velocity are free (and is not restricted to periodic trajectories). A strategy is presented for the case when the input is bounded. Robustness for this class of hybrid strategies is also investigated both numerically and analytically for different types of disturbances and uncertainties (measurement noise,

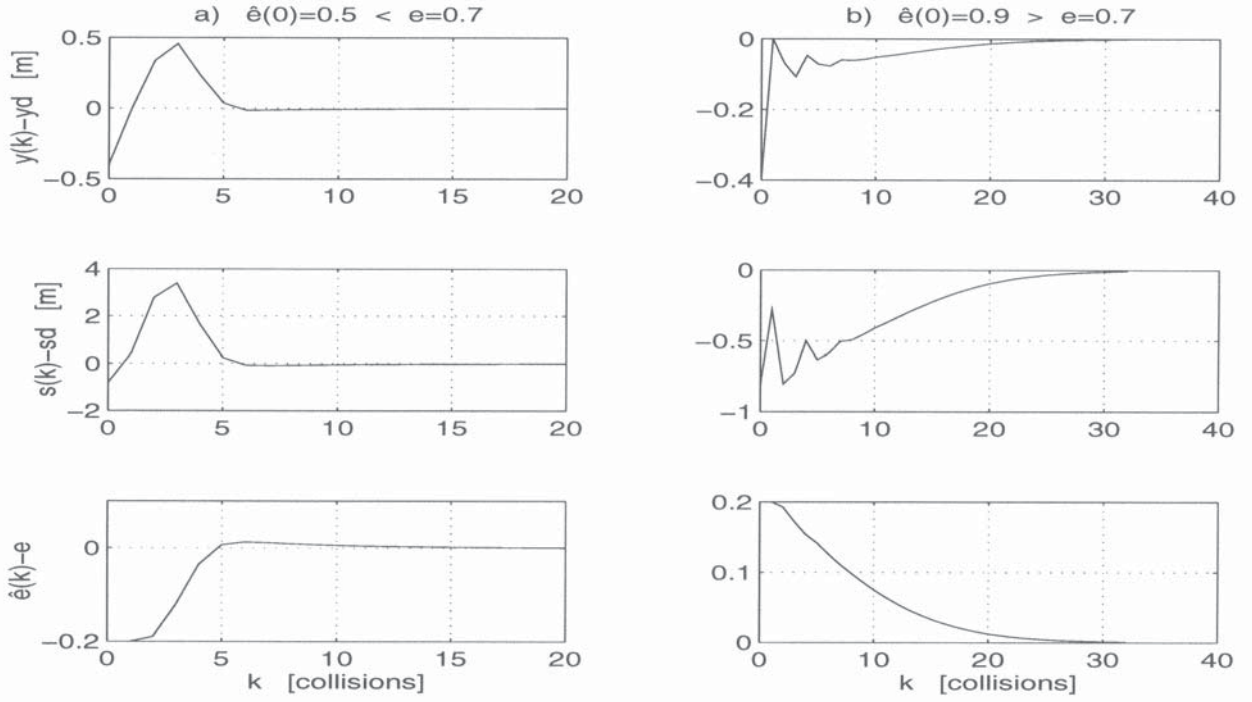


Figure 8. Adaptation errors: a) $\hat{e}(0) < e$; b) $\hat{e}(0) > e$.

bad knowledge of the restitution coefficient, unknown damping on the object during the flight-times). The possible extension of the presented method to a larger class of mechanical systems with unilateral constraints is also outlined.

A. Proof of Claim 1

The proof is divided in two parts: In *Part 1* we treat the generic case in which $e \in (0, 1]$ and an initial impact takes place at $t_0 \geq 0$, i.e., $y_1(t_0) - y_2(t_0) = 0$ and $\dot{y}_1(t_0^+) - \dot{y}_2(t_0^+) > 0$. In *Part 2* we suppose that the two bodies are in contact at a generic instant t_k (in which the control input (17)–(24) is applied), i.e., $y_1(t_k) - y_2(t_k) = \dot{y}_1(t_k) - \dot{y}_2(t_k) = 0$. The objective of *Part 2* is to prove that points 1–4 of claim 1 are true also for the perfectly plastic case, i.e., $e = 0$, and for the case in which the bodies are in contact at t_0 (for any value of $e \in [0, 1]$).

Part 1. Let us for the moment consider the isolated dynamics of the ball (5) assuming initial conditions $(y_1(t_k), \dot{y}_1(t_k)) = (y(k), \dot{y}_1(k))$. Then, it is easy to verify that the position and velocity after a time interval d_k as defined in (21) are

$$(y_1(t_k + d_k), \dot{y}_1(t_k + d_k)) = \left(y^*(k + 1), -\sqrt{\dot{y}_1^2(k) - 2g(y^*(k + 1) - y(k))} \right) \quad (50)$$

for any $y^*(k + 1)$ satisfying (23). Notice that (23) determines the set of reachable positions of the ball given specific initial states. This condition not only ensures that the term in the square roots of (21) and (50) (see also (22)) is non-negative but also ensures positive values of d_k . Complex or negative time intervals would not make any sense.

Now, let us consider the isolated dynamics of the surface. From (6) and (17), one obtains $\ddot{y}_2 = v$. This system is easily written as

$$\dot{z} = Fz + Gv \quad (51)$$

for suitable (F, G) and z . Then, the control input

$$v(t) = G^T \Gamma^T(-t) W^{-1} \Gamma(-t_k - d_k) [z_{k+1} - \Gamma(d_k) z_k] \quad (52)$$

where

$$W = \int_{t_k}^{t_k+d_k} \Gamma(-\tau) G G^T \Gamma^T(-\tau) d\tau \quad (53)$$

and $\Gamma(t) = \exp(Ft)$ are respectively the Gramian and the state-transition matrix of (51), drives the state z from z_k to z_{k+1} in the time interval d_k (see [31]). Such controllers are sometimes called *Dead-beat* algorithms [18]. Choosing $z_k^T = (y(k), \dot{y}_2(k))$ and $z_{k+1}^T = (y^*(k+1), \dot{y}_2^*(k+1))$ in (52), we get (18)–(20) as the input that leads the surface states from $(y_2(t_k), \dot{y}_2(t_k)) = (y(k), \dot{y}_2(k))$ to

$$(y_2(t_k + d_k), \dot{y}_2(t_k + d_k)) = (y^*(k+1), \dot{y}_2^*(k+1)) \quad (54)$$

Notice that the d_k used in (19) and (20) is designed using (21) which makes the final position of the isolated trajectory of the surface coincide with the one of the ball. In other words, $y_1(t_k + d_k)$ and $y_2(t_k + d_k)$ in (50) and (54) satisfy

$$y_1(t_k + d_k) = y_2(t_k + d_k) = y^*(k+1) \quad (55)$$

Let us now consider the whole dynamics (5)–(8) assuming initial conditions such that $y_1(k) \equiv y_2(k) \equiv y(k)$ and

$$\dot{y}_1(k) - \dot{y}_2(k) > 0 \quad (56)$$

Notice that these are in general the conditions that result of an impact when $e \in (0, 1]$. Introducing (17), (18) in (6) and integrating two times (5) and (6) for $t \in (t_k, t_k + d_k)$, we get

$$f(y_1(t), y_2(t)) \triangleq y_1(t) - y_2(t) = -\Delta \left[\frac{A_k}{6} \Delta^2 + \frac{B_k + g}{2} \Delta + (\dot{y}_2(k) - \dot{y}_1(k)) \right] \triangleq f(\Delta) \quad (57)$$

where $\Delta \triangleq t - t_k$. It is not difficult to verify that (57) can be rewritten as

$$f(\Delta) = -\Delta (\Delta - d_k) Y(\Delta) \quad (58)$$

where $Y(\Delta) = \frac{A_k}{6} \Delta + \frac{A_k}{6} d_k + \frac{B_k + g}{2}$. From (19) and (20), and considering conditions (56) and (24), one can verify that $Y(\Delta) > 0, \forall \Delta \in (0, d_k)$. From this fact, one easily sees that

$f(\Delta) > 0, \forall \Delta \in (0, d_k)$, which demonstrates point 1 of the claim. This and (55) prove points 2 and 3.

Finally, from (5)–(8) it follows that at a generic impact $k + 1$

$$\dot{y}_1(k + 1) = \frac{m - e}{1 + m} \dot{y}_1(t_{k+1}^-) + \frac{1 + e}{1 + m} \dot{y}_2(t_{k+1}^-) \quad (59)$$

$$\dot{y}_2(k + 1) = \frac{m(1 + e)}{1 + m} \dot{y}_1(t_{k+1}^-) + \frac{1 - em}{1 + m} \dot{y}_2(t_{k+1}^-) \quad (60)$$

Considering (50) and (54) in (59), one gets

$$\dot{y}_1(k + 1) = -\frac{m - e}{1 + m} \sqrt{\dot{y}_1^2(k) - 2g(y^*(k + 1) - y(k))} + \frac{1 + e}{1 + m} \dot{y}_2^*(k + 1) \quad (61)$$

Introducing (22) into (61), point 4 follows.

Part 2. Let us now suppose that at a generic instant t_k , both bodies are in contact and tend to move together, i.e.,

$$y_1(t_k) - y_2(t_k) = \dot{y}_1(t_k) - \dot{y}_2(t_k) = 0 \quad (62)$$

Notice that this may be the result of two possible situations: On the one hand, when the restitution coefficient is zero, i.e., $e = 0$, (62) takes place at impact instants t_k (see (8)). In the other hand, when the two bodies are in contact at the initial instant t_0 , (62) is verified with $k = 0$. Notice that this last situation does not depend on the value of e .

Considering this assumption, and from (1)–(3), the system dynamics becomes

$$m_1 \ddot{y}_1 + m_1 g = \lambda \quad (63)$$

$$m_2 \ddot{y}_2 + m_2 g = u - \lambda \quad (64)$$

$$f(y_1, y_2) = y_1 - y_2 = 0 \quad (65)$$

where $\lambda > 0$ is the interaction force between the bodies. This dynamics holds until the moment t' in which the interaction force vanishes and the relative acceleration becomes positive, i.e., $\lambda(t') = 0$ and $\ddot{y}_1(t') - \ddot{y}_2(t') > 0$. From (63) and (64), it is easy to verify that this condition is translated to: $\ddot{y}_1(t') - \ddot{y}_2(t') = \left(\frac{1}{m_1} + \frac{1}{m_2}\right) \lambda(t') - \frac{u(t')}{m_2} = -\frac{u(t')}{m_2} > 0$, i.e., $u(t') < 0$. Considering the input force (17)–(24) taking into account (62), we can prove that $u(t_k^+) = m_2(g + B_k) < 0$ (see [39], app. B, sect. B.2). We conclude that $t' = t_k^+$, that is, the bodies loose contact at the immediate instant in which the control input (17)–(24) is applied (just after the shocks for the perfectly plastic case). The dynamics in (5)–(8) is recovered at $t = t' = t_k^+$. Consequently, *Part 1* of the proof holds for this case too.

Acknowledgments

A. Zavala Río was supported by CONACYT-Mexico. Part of this work was performed while he held a post-doctoral fellowship at the Mechanical Engineering Laboratory, AIST, Japan.

Notes

1. For instance the work in [8] for stabilization of hopping robots strongly relies on the choice $e = 0$ which allows them to apply a control during the constrained motion phase. It is not clear how the results can be extended to the case $e > 0$.
2. It would be indeed difficult to think of the case in which the collisions are perfectly elastic while one tries to model them as perfectly plastic.

References

1. Aboaf, E. W., Drucker, S. M. and Atkeson, C. G., "Task-level robot learning: Juggling a tennis ball more accurately," in *IEEE International Conference on Robotics and Automation*, Scottsdale, Arizona, pp. 1290–1295, 1989.
2. Brach, R. M., *Mechanical Impact Dynamics, Rigid Body Collisions*, New York: Wiley Interscience Publications, John Wiley and Sons, 1991.
3. Branicky, M. S., Borkar, V. S. and Mitter, S. K., "A unified framework for hybrid control: Background, model and theory," in A. Bensoussan and J. L. Lions, editors, *International Conference on Analysis and Optimization of Systems*, France, pp. 352–358, 1994. INRIA. Also in *IEEE Conference on Decision and Control*, Lake Buena Vista, Florida, pp. 4228–4234, 1994.
4. Brogliato, B., Niculescu, S. I. and Orhant, P., "On the control of finite dimensional mechanical systems with unilateral constraints," *IEEE Transactions on Automatic Control*, vol. 42, pp. 200–215, 1997.
5. Buehler, M., *Robotic tasks with intermittent dynamics*, PhD thesis, Yale University, New Haven, 1990.
6. Buehler, M., Koditschek, D. E. and Kindklmann, P. J., "A family of robot control strategies for intermittent dynamical environments," *IEEE Control Systems Magazine*, vol. 10, pp. 16–22, 1990.
7. Buehler, M., Koditschek, D. E. and Kindklmann, P. J., "Planning and control of robotic juggling and catching tasks," *International Journal of Robotics Research*, vol. 13, pp. 101–118, 1994.
8. François, C., *Contribution à la locomotion articulée dynamiquement stable*, PhD thesis, École des Mines de Paris, Sophia Antipolis, France, 1996.
9. Guckenheimer, J. and Holmes, P., *Nonlinear Oscillations, Dynamical Systems and Bifurcations of Vector Fields*, New York: Springer-Verlag, 1983.
10. Hemami, H. and Wyman, B., "Modelling and control of constrained dynamic systems with application to biped locomotion in the frontal plane," *IEEE Transactions on Automatic Control*, vol. 24, pp. 526–535, 1979.
11. Higuchi, T., "Application of electro-magnetic impulsive force to precise positioning tools in robot systems," in *2nd. International Symposium on Robotics Research*, Cambridge, Massacusetts: MIT Press, 1985, pp. 281–285.
12. Hindmarsh, M. B. and Jefferies, D. J., "On the motions of the offset impact oscillator," *Journal of Physics A: Math. Gen.*, vol. 17, pp. 1791–1803, 1984.
13. Holmes, P. J., "The dynamics of repeated impacts with a sinusoidally vibrating table," *Journal of Sound and Vibrations*, vol. 84, pp. 173–189, 1982.
14. Huang, H. P. and McClamroch, N. H., "Time optimal control for a robotic contour following problem," *IEEE Journal of Robotics and Automation*, vol. 4, pp. 140–149, 1988.
15. Huang, W., Krotkov, E. P. and Mason, M. T., "Impulsive manipulation," in *IEEE International Conference on Robotics and Automation*, Nagoya, Japan, pp. 120–125, 1995.
16. Hurmuzlu, Y., "Dynamics of bipedal gait. Part 1: Objective functions and the contact event of a planar 5-link biped. Part 2: Stability analysis of a planar 5-link biped," *ASME Journal of Applied Mechanics*, vol. 60, pp. 331–334, 1993.
17. Kolmanovsky, I. and McClamroch, N. H., "Hybrid feedback laws for a class of cascade nonlinear control systems," *IEEE Transactions on Automatic Control*, vol. 41, 1996.
18. Kreisselmeier, G. and Lozano, R., "Adaptive control of continuous-time overmodeled plants," *IEEE Transactions on Automatic Control*, vol. 41, pp. 1779–1794, 1996.

19. Lynch, K. M. and Mason, M. T., "Stable pushing: mechanics, controllability, and planning," *International Journal of Robotics Research*, vol. 15, pp. 533–556, 1996.
20. Masri, S. F. and Caughey, T. K., "On the stability of the impact damper," *ASME Journal of Applied Mechanics*, vol. 33, pp. 586–592, 1966.
21. Peshkin, M. A. and Sanderson, A. C., "Planning robotic manipulation strategies for workpieces that slide," *IEEE Journal of Robotics and Automation*, vol. 4, pp. 524–531, 1988.
22. Rizzi, A. A. and Koditschek, D. E., "Preliminary experiments in robot juggling," in *International Symposium on Experimental Robotics*, Toulouse, France, 1991. MIT Press.
23. Rizzi, A. A. and Koditschek, D. E., "Progress in spatial robot juggling," in *IEEE International Conference on Robotics and Automation*, Nice, France, pp. 775–780, 1992.
24. Rizzi, A. A. and Koditschek, D. E., "Further progress in robot juggling: the spatial two-juggle," in *IEEE International Conference on Robotics and Automation*, Atlanta, Georgia, pp. 919–924, 1993.
25. Rizzi, A. A. and Koditschek, D. E., "Further progress in robot juggling: solvable mirror laws," in *IEEE International Conference on Robotics and Automation*, San Diego, California, pp. 2935–2940, 1994.
26. Rizzi, A. A. and Koditschek, D. E., "An active visual estimator for dexterous manipulation," *IEEE Transactions on Robotics and Automation*, vol. 12, pp. 697–713, 1996.
27. Rizzi, A. A., Whitcomb, L. L. and Koditschek, D. E., "Distributed real-time control of a spatial robot juggler," *IEEE Computer*, vol. 25, pp. 12–24, 1992.
28. Schaal, S. and Atkeson, C. G., "Open loop stable control strategies for robot juggling," in *IEEE International Conference on Robotics and Automation*, Atlanta, Georgia, pp. 913–918, 1993.
29. Schaal, S. and Atkeson, C. G., "Robot juggling: implementation of memory based learning," *IEEE Control Systems*, pp. 57–71, 1994.
30. Shaw, S. W., and Rand, R. H. "The transition to chaos in a simple mechanical system," *International Journal of Non-linear Mechanics*, vol. 24, pp. 41–56, 1989.
31. Sontag, E. D. *Mathematical Control Theory, Deterministic Finite Dimensional Systems*. TAM 6. Springer-Verlag, 1990.
32. ten Dam, A. A. "Representations of dynamical systems described by behavioral inequalities," in *European Control Conference*, Groningen, Netherlands, pp. 1780–1783, 1993.
33. ten Dam, A. A., Dwarshuis, E. and Willems, J. C., "The contact problem for linear continuous-time dynamical systems: A system theoretical approach," *IEEE Transactions on Automatic Control*, vol. 42, pp. 458–472, 1997.
34. van der Schaft, A. J. and Schumacher, J. M., "The complementary-slackness class of hybrid systems," *Mathematics of Control Signals and Systems*, vol. 9, pp. 266–301, 1996.
35. Vincent, T. L., "Controlling a ball to bounce at a fixed height," in *American Control Conference*, Seattle, Washington, pp. 842–846, 1995.
36. Vincent, T. L., "Controllable targets on or near a chaotic attractor," in *Control and Chaos*, Birkhauser, 1997.
37. Wang, Y., "Dynamics and planning of collisions in robotic manipulation," in *IEEE International Conference on Robotics and Automation*, Scottsdale, Arizona, pp. 478–483, 1989.
38. Wang, Y., "Dynamic modeling and stability analysis of mechanical systems with time-varying topologies," *ASME Journal of Mechanics Design*, vol. 115, pp. 808–816, 1993.
39. Zavala-Río, A., *Commande de robots jongleurs*, PhD thesis, Laboratoire d'Automatique de Grenoble, ENSIEG, INPG, France, 1997.
40. Zavala-Río, A. and Brogliato, B., "Hybrid feedback strategies for the control of juggling robots," in *Proceedings of the Workshop Modelling and Control of Mechanical Systems*, London, U.K., pp. 235–251, 1997. Imperial College Press.
41. Zavala-Río, A. and Brogliato, B., "On the feedback control of a simple juggling robot," in *European Control Conference*, Brussels, Belgium, 1997. Paper No. 871.
42. Zavala-Río, A. and Brogliato, B., "Robust control of one degree-of-freedom jugglers," in *IFAC 5th Symposium on Robot Control*, Nantes, France, pp. 703–708, 1997.
43. Zumel, N. B. and Erdmann, M. A., "Balancing of a planar bouncing object," in *IEEE International Conference on Robotics and Automation*, San Diego, California, pp. 2949–2954, 1994.